Spin-resolved photoemission of *in situ* sputtered iron and iron-yttrium alloys

Y. B. Xu and D. Greig

Department of Physics & Astronomy, The University of Leeds, Leeds, LS2 9JT, United Kingdom

E. A. Seddon

Daresbury Laboratory, Daresbury, Warrington, Cheshire, WA4 4AD, United Kingdom

J. A. D. Matthew

Department of Physics, The University of York, Heslington, York, YO1 5DD, United Kingdom
(Received 9 September 1996; revised manuscript received 11 November 1996)

Spin-resolved photoemission spectra of amorphous Fe-Y alloys have been obtained and compared with both those of pure Fe and with theoretical electronic structure calculations. The thin iron and alloy films were prepared by *in situ* sputtering, and the spectra were obtained using 110-eV photons from the UK Synchrotron Facility. From secondary electron spin hysteresis loops, $Fe_{60}Y_{40}$ starts to order ferromagnetically well before the lowest temperature accessible with our equipment (114 K), but $Fe_{41}Y_{59}$ shows no polarization down to this temperature. Although the spin-integrated photoemission spectrum of the valence band of $Fe_{60}Y_{40}$ shows little difference from that of pure Fe, the spin-resolved spectra are significantly different. $Fe_{60}Y_{40}$ also exhibits a reduced valence band polarization (14%) compared with iron, and contrary to predictions, the majority spin states of $Fe_{60}Y_{40}$ dominate at the Fermi edge. No evidence is found for strong ferromagnetism. Unexpectedly, the 1-eV secondary electron polarization of $Fe_{60}Y_{40}$ (7%) is found to be low compared with the valence band polarization, an effect that may be due to a negative moment on the yttrium. [S0163-1829(97)03017-8]

I. INTRODUCTION

Amorphous alloys based on iron and yttrium are particularly interesting from a fundamental point of view as a range of Fe-Fe spin interactions are predicted across the composition range.[1] In addition, they are of interest to theorists as they serve as models for transition-metal–rare-earth alloys without the complications that arise from a large localized $4f$ moment. Recently, there has been a surge in activity among the theoretical community and a number of reports of the spin-dependent electronic structure of amorphous alloys have appeared in the literature.[1–6] These predictions can now be tested in a very direct manner using spin-resolved photoemission (SRPE). The structural, electronic, and magnetic properties of Fe-Y alloys in particular have been predicted by Yu and Kakehashi[2] and by Becker and Hafner.[1] These latter authors predict chemical short-range order for all compositions and that the local topology at short distances is very similar in both the crystalline and glassy phases. Several notable features emerged from the calculations. For example, at Fe concentrations of greater than 80% competing ferromagnetic and antiferromagnetic spin interactions lead to a predicted coexistence of positive and negative Fe moments. The Y atoms carry small negative moments that persist even into the Fe-rich regime. With increasing Y concentration, the valence band of the alloys narrows and the systems approach a transition from weak to strong ferromagnetism. Though not reporting the fundamental electronic structure of Fe-Y alloys in the depth of the Hafner study, the findings of Yu and Kakehashi[2] are broadly similar to those outlined above, apart from predictions for alloys with a very high iron content, i.e., >90% Fe.

In our previous experimental studies on amorphous alloys, as in all previous SRPE experimental work on these materials,[7–9] the amorphous alloys were in the form of ribbons produced by melt spinning. The samples were then transferred to a UHV chamber where they were mounted onto a specially designed sample holder for the measurements. The preparation technique and the transportation of the samples meant that extensive cleaning was required, and it was found that the carbon contamination levels could only be minimized rather than reduced to undetectable levels. This latter is a well-documented finding by several groups.[9–11] For amorphous alloys, a broader composition range is usually accessible using sputtering rather than melt spinning owing to the much higher quenching rate of the sputtering technique. An *in situ* sputter preparation technique was therefore a highly desirable goal. As a result, we have prepared two representative samples of Fe-Y alloys, as well as pure Fe, by *in situ* sputtering, with the aims of gaining an insight into their electronic and magnetic structure and of testing some of the theoretical predictions discussed above.

II. EXPERIMENT

The spin-polarized photoemission work reported here was performed on station 6.1 of the Synchrotron Radiation Source (SRS) at Daresbury Laboratory. The station, which is designed for UHV (base pressure 2×10^{-10} mbar) photoemission work over the photon energy range 80–180 eV, was modified for this spin-resolved work by the incorporation of a small hemispherical energy analyzer and "micro-Mott" polarimeter. This equipment is described in detail elsewhere.[12,13] An effective Sherman function of 0.12 was established for the polarimeter (operating at 20 kV with an
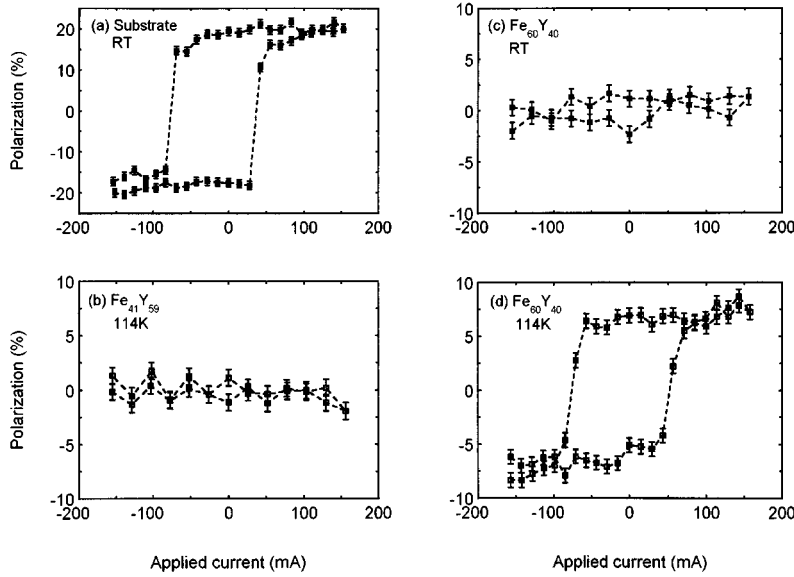
FIG. 1. Photon (110 eV) initiated 1 eV spin asymmetry hysteresis loops of (a) $Co_{77}B_{23}$ ribbon substrate at room temperature (RT), (b) $Fe_{41}Y_{59}$ ($\sim$50 Å)/$Co_{77}B_{23}$ at low temperature (114 K), (c) $Fe_{60}Y_{40}$ ($\sim$50 Å)/$Co_{77}B_{23}$ at room temperature, and (d) $Fe_{60}Y_{40}$($\sim$50 Å)/$Co_{77}B_{23}$ at low temperature (114 K).

energy window of 400 V) by assuming that the 20 eV secondary electron polarization of Fe is 27%.[14]

From an experimental point of view, sputter-grown materials present a number of challenges because samples for study by spin-polarized electron spectroscopy should ideally exhibit a large remanent magnetization and (to minimize any stray magnetic fields) they should be formed into closed loops, the magnetization direction of which can easily be reversed. Cooling of the samples is also desirable in many instances. These critical requirements may be why experimental investigations, as opposed to theoretical calculations, of the spin-dependent electronic structure of amorphous materials are rare.

In order to achieve these objectives and to make possible the study of a range of materials in a single run without breaking the vacuum, a preparation chamber (base pressure 3×10^{-10} mbar) was attached to the main chamber, and a manipulator end piece and sample holder were specially designed (experimental details will be published elsewhere[15]). The thin film samples were prepared by cosputtering on an amorphous alloy substrate ($Co_{77}B_{23}$) that was already formed into a closed loop with an attached magnetizing coil. The exchange interaction between the substrate and the sputter-grown film then ensures that an easily achievable field is required for the magnetization reversal. Dynamic sample cooling was achieved using liquid nitrogen. The compositions Fe_xY_{1-x} of two samples were obtained by choosing the deposition rates of each target and found to be $x=0.41\pm0.06$ and 0.60 ± 0.06, respectively, from the relative intensities of the Fe:$3p$/Y:$4p$ photoemission intensities with 140 eV photons using the cross sections reported by Yeh and Lindau.[16] The film thicknesses were estimated using a crystal oscillator positioned approximately 3 cm behind and slightly above the sample position. No Co core-level peaks were visible after sample depositions.

Although the thinness and chemical reactivity of the Fe-Y films grown in this study precluded direct experimental confirmation of their amorphous nature, Coey *et al.* have shown by x-ray diffraction that thicker sputter-grown films of Fe_xY_{1-x} ($x=0.32-0.88$) are amorphous.[17]

The substrate ribbon was made by melt spinning, and *ex*

situ magneto-optical Kerr effect measurements showed (i) that it could be magnetized to saturation by passing a small current through the insulated coil and (ii) that it exhibits 100% remanence. After deposition (onto the shiny side of the ribbon), the whole sample plate was transferred from the preparation chamber to the adjoining main chamber in a maneuver taking only a few minutes and without compromising the system vacuum. A -20 V sample bias was applied to ensure that only those electrons originating in the sample were detected.

III. RESULTS

Figure 1 shows a reproducible set of four hysteresis loops obtained from the spin asymmetry of 1 eV secondary electrons following excitation by 110 eV photons. The four diagrams are (a) $Co_{77}B_{23}$ ribbon substrate at room temperature (RT), (b) $Fe_{41}Y_{59}$($\sim$50 Å)/$Co_{77}B_{23}$ at low temperature (114 K), (c) $Fe_{60}Y_{40}$($\sim$50 Å)/$Co_{77}B_{23}$ at room temperature, and (d) $Fe_{60}Y_{40}$($\sim$50 Å)/$Co_{77}B_{23}$ at low temperature (114 K).

Figure 1(a) clearly shows that the $Co_{77}B_{23}$ substrate can be magnetized to saturation at room temperature with an applied current smaller than 100 mA (the magnetic field at this current is about 0.1 Oe for the three-turn coil used). The remanence ratio is close to 100% and the polarization is $\sim$20%. Upon room-temperature sputter deposition of approximately 50 Å of $Fe_{60}Y_{40}$, the polarization was found to reduce to close to zero. However, as the temperature of the sample plate was reduced to the lowest value accessible with our equipment, around 114 K, a clear 7 ± 1 % polarization signal emerged. This result again demonstrates the utility of employing the ''internal field ($\sim10^7$ Oe)'' of the magnetic substrate to magnetize thin films as bulk iron-yttrium alloys are normally only magnetized with very high external fields (10^4-10^5 Oe).[18,19] As expected, the low-temperature hysteresis loop of $Fe_{60}Y_{40}$ shows almost the same coercive field as that of the substrate, but it exhibits a reduced polarization. However, it is important to note that any domain structure present in the $Co_{77}B_{23}$ substrate may be mirrored in the Fe-Y film. Van Zandt *et al.* have demonstrated that substrate domain features are visible in Fe overlayers up to 25–30 Å
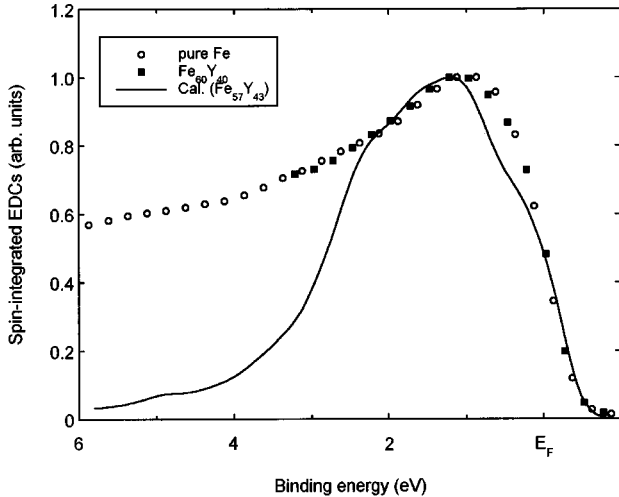
FIG. 2. Spin-integrated energy distribution curves (EDC's) of pure Fe and $Fe_{60}Y_{40}$, both obtained at a photon energy of 110 eV. The dots are experimental results, and the line is the theoretical EDC of $Fe_{57}Y_{43}$ by Becker and Hafner (Ref. 1).

FIG. 3. Valence-band photoelectron spin-polarization spectra of pure Fe and $Fe_{60}Y_{40}$ (photon energy 110 eV).

thick. Indeed, they have used this effect to enhance very-low-contrast scanning electron microscopy with polarization analysis (SEMPA) images.[20]

Although we cannot exclude the possibility of a hysteresis contribution associated with the remanence of blocked superparamagnetic Fe precipitates,[21] the shape of the observed hysteresis loop supports the presence of a dominant ferromagnetic phase. The results also exclude the possibility that the material is polycrystalline $Fe_{60}Y_{40}$ for which a Curie temperature of ~550 K is expected.[18,22] In contrast, a polarization signal was not observed for the Y-rich alloy [see Fig. 1(b)], showing that the $Fe_{41}Y_{59}$ alloy is either in a paramagnetic or an antiferromagnetic state for temperatures from room temperature down to 114 K.

Figure 2 shows the spin-integrated energy distribution curves (EDC's) of $Fe_{60}Y_{40}$ and Fe, both obtained at a photon energy of 110 eV. The alloy spectra were collected over a narrower energy range than that of Fe to shorten the collection time and minimize the effects of oxidation. However, the chosen energy range is expected to reflect the main features of the valence band. As the Y $4d$ cross section is much smaller than the Fe $3d$ cross section at the photon energy used [Y(0.037)/Fe(4.02)~10^{-2} (Ref. 16)], the EDC of Fe-Y is expected to be dominated by the Fe states. It is interesting that the spin-integrated EDC's of Fe and $Fe_{60}Y_{40}$ are very similar, both exhibiting a peak at ~1 eV binding energy. The x-ray photoemission spectra (XPS) of amorphous $Fe_{35}Y_{65}$ and $Fe_{79}Y_{21}$ have been reported by Tenhover et al.[23] and Conell et al.[24]—in both cases, the spectra obtained also showed a maximum intensity at 1 eV binding energy. Clearly, it is difficult to discern the possible differences of the iron d band in pure Fe and Fe-Y amorphous alloys from spin-integrated measurements. The solid line in Fig. 2 is the calculated EDC of $Fe_{57}Y_{43}$ (from Becker and Hafner[1]) convoluted with an instrumental broadening function of 0.6 eV and shifted by 0.2 eV in order to align the Fermi edge with the experimental points. The calculated and experimental results are in reasonable agreement up to 3 eV binding energy before loss processes make a comparison difficult. However,
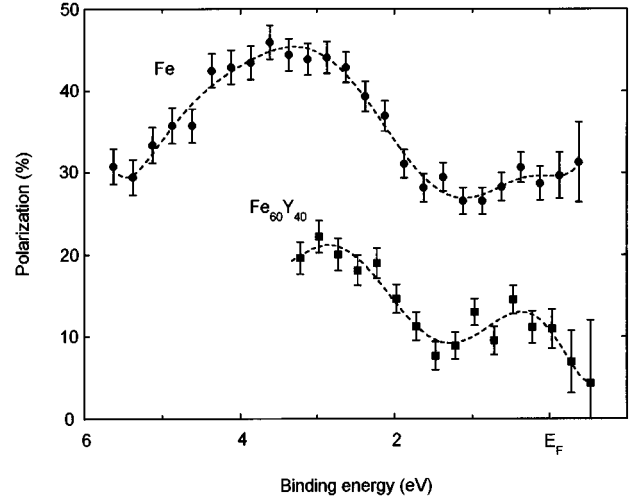
there are significant deviations in the near-Fermi-edge region.

Figure 3 shows the valence-band spin-polarization spectra of $Fe_{60}Y_{40}$ and of pure Fe excited with 110 eV photons. The polarization of Fe was measured at room temperature, while that of $Fe_{60}Y_{40}$ was obtained at 114 K. The polarization spectrum of Fe shows a broad peak at around 3 eV and a shallow minimum at about 1 eV. Though the polarization spectrum of the $Fe_{60}Y_{40}$ has a similar profile to that of pure Fe, there are also significant differences, the most pronounced of which is that over the full range measured the observed polarization of the alloy is much smaller than that of Fe. In addition, the polarization spectrum of $Fe_{60}Y_{40}$ shows evidence of a new peak at about 0.4 eV binding energy and a rapidly diminishing polarization near E_f. This latter is probably due to a shift (compared with Fe) of the peak of the minority spin states to higher binding energies, resulting in greater occupation.

The spin-resolved EDC's of Fe and $Fe_{60}Y_{40}$ are shown in Fig. 4(a), and the experimental spin-resolved EDC's of $Fe_{60}Y_{40}$ are compared with the theoretical spin resolved EDC's of amorphous $Fe_{57}Y_{43}$ (Ref. 1) in Fig. 4(b). In both of these figures, the estimated experimental errors are comparable to the size of the data points. From Fig. 4(a), the majority-spin spectrum of Fe exhibits a weak maxima around ~3 eV in addition to a main peak at ~1.0 eV. The minority-spin spectrum has only a single peak at ~1.0 eV. This indicates an effective exchange splitting of ~2 eV for pure Fe, consistent with the values of 1.9±0.2 eV (Ref. 8) and ~2.0 eV (Ref. 25) reported for polycrystalline iron. The Fe spectra in Fig. 4(a) also have a very similar profile to those of evaporated polycrystalline Fe.[25] For $F_{60}Y_{40}$, the separation of the majority-spin states and the minority-spin states is clearly much smaller, implying reduced effective exchange splitting.

IV. DISCUSSION

A. Secondary electron polarization

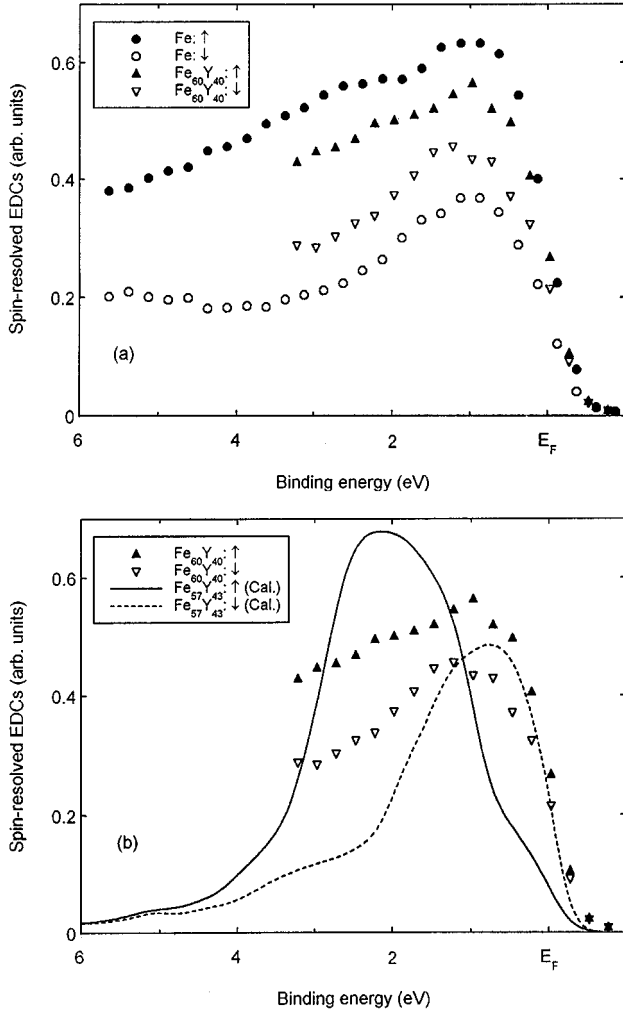The 1 eV secondary electron polarizations of Fe and $Fe_{60}Y_{40}$ are displayed in Table I, along with the average

FIG. 4. (a) Spin-resolved EDC's of pure Fe and $Fe_{60}Y_{40}$ and (b) comparison of the experimental EDC's of $Fe_{60}Y_{40}$ and the theoretical spin-resolved EDC's of $Fe_{57}Y_{43}$ by Becker and Hafner (Ref. 1).

were constant. The P_{SE}/P_{VB} ratio is therefore independent of the choice of sample, substrate, and Sherman function.

Considering the Fe data first, we note that the secondary electron polarization shows the expected behavior for transition metals or alloys[14,26] in that the 1 eV secondary electrons have an electron polarization significantly higher than that of the average VB polarization (an effect due to spin-dependent transport of the secondary electrons with less than 10 eV kinetic energy). In contrast, the 1 eV secondary electrons of $Fe_{60}Y_{40}$ have both much lower absolute polarization than that of Fe and a lower value than that of the valence band of $Fe_{60}Y_{40}$. Given the well-behaved electron emission from iron, the low values for $Fe_{60}Y_{40}$ (recorded under identical experimental conditions) cannot be attributed to instrumental effects, such as spin precession of low kinetic-energy electrons due to stray fields.

Although the moderate energy (10–20 eV) secondary electron polarization is often equated with the mean valence band polarization, these are quite different quantities and the polarizations obtained may differ for a number of reasons. In the context of this study, the most important of these are cross section effects. As discussed above, at 110 eV photon energy the valence band photoemission of Fe-Y is dominated by the Fe 3d electrons rather than being a true reflection of both the Fe- and Y-based density of states. The secondary electron cascade region involves much lower-energy transitions from spin-dependent filled states to empty states that may also be polarized. Transitions from Y 4d states will now be far more prominent as the Y contribution is no longer suppressed by a low cross section; in addition, contributions from s and p electrons may also be significant. If Y in $Fe_{60}Y_{40}$ does exhibit negative moments, as predicted by Becker and Hafner [$\sim -0.4\mu_B$ (Ref. 1)], this factor will be important in determining the absolute value of the low-energy secondary electron polarization.

A diminution rather than an enhancement of polarization at very low secondary electron energies has been observed previously for gadolinium deposited on W(110).[27,28] This result was rationalized by assuming that, in addition to scattering into the available conduction band states (of either spin character), very low-energy minority-spin electrons can also scatter into the fully polarized vacant Gd 4f state that lies approximately 1 eV above the vacuum level. Comparable vacant states are not available in Fe-Y (although complexities in the character of empty conduction band states could lead to similar effects), suggesting that the small magnitude of the 1 eV secondary electron polarization in Fe-Y is due primarily to negative moments on the Y atoms.

polarization of the valence band (VB) photoemission calculated from the spin-resolved EDC's shown in Fig. 4(a). Also included in the table are those values for Fe reported in the literature. When considering the data obtained in this study, it is important to note that both the secondary electron and the valence band values for each material were obtained on the same sample, the Fe and $F_{60}Y_{40}$ films were grown on the same substrate, and the polarimeter operating conditions

TABLE I. 1 eV secondary electron and average valence band polarizations (%).

Sample	$P_{1 \text{ eV SE}}$	P_{VB}	Photon energy (eV)	Temperature (K)	Ref.
Fe	44±2	34±2	110	RT	This work
Fe(100)	45±5		60	RT	31
Fe(100)	46		500	RT	32
Fe polycrystalline		25±2	1256	RT	8
Fe polycrystalline		34	260	RT	25
$Fe_{60}Y_{40}$	7±1	14±1	110	114	This work

B. Valence band photoemission

Consider first the average valence band polarization in Table I. One interesting feature is the reduction in polarization of pure Fe observed on changing from soft x-ray radiation [110 and 260 eV (Ref. 25)] to Mg $K\alpha$ [1256 eV (Ref. 8)] radiation. The measurement reported by Sinkovic et al.[25] was determined by spin-polarized photoemission using 260 eV photons and is similar to the value obtained in this study (110 eV). That of See and Klebanoff,[8] obtained using Mg $K\alpha$ radiation, is significantly smaller. Although some of the difference will, no doubt, be due to Sherman function uncertainties, two effects, the cross section and the probing depth dependences on electron kinetic energy, are proposed to be primarily responsible for this result.

The photon energy dependence of the cross sections of iron $3d$ and $4s$ electrons is given by Yeh and Lindau,[16] and from their values we obtain $\sigma_{4s}/\sigma_{3d} = 0.012$, 0.022, and 0.21 for 110, 260, and 1254 eV photons, respectively. If the $4s$ electrons are essentially unpolarized, the calculated and observed trends are in agreement. If the s electrons are in fact negatively spin polarized, as suggested from neutron scattering[29] and Compton scattering experiments,[30] the influence of the cross section effect will be further enhanced. A higher Fe P_{VB} for photoemission using soft x rays as opposed to Mg $K\alpha$ radiation is also expected if there is a moment enhancement at the surface of the sample because the probing depth of soft x-ray photoemission is much smaller than that of x-ray photoemission. Evidence for surface moment enhancement has recently been presented by Sinkovic et al.[25]

The experimental spin-resolved EDC's of $Fe_{60}Y_{40}$ [Fig. 4(b)] show different features from those calculated for $Fe_{57}Y_{43}$, the closest alloy composition for which theoretical results are available. Broadening of the theoretical density of states (DOS) of amorphous $Fe_{57}Y_{43}$ (Ref. 1) by a 0.6 eV instrumental function to simulate finite experimental resolution effects allows (with minor reservations) a direct comparison of the theoretical and experimental data [see Fig. 4(b)]. The theoretical work suggests that increasing the Y concentration in Fe-Y alloys leads to diminishing band splitting and narrowing d-band widths and, in the Y-rich regime, approaches a transition from weak to strong ferromagnetism. The theoretical spin-resolved EDC's of $Fe_{57}Y_{43}$ (Ref. 1) each show only a single peak together with low-intensity shoulders, and the minority states clearly dominate around E_f. Experimentally, the majority-spin photoelectrons do not decrease rapidly in intensity as E_f is approached—indeed, they are still dominant at E_f as clearly shown in Figs. 3 and 4(a). The discrepancy cannot be resolved by poor energy resolution as convoluting the theoretical predictions with a 2 eV resolution function still results in a predicted negative polarization at E_f.

The disagreement between the spin-resolved experimental and theoretical EDC's is essentially a discrepancy in the bonding and antibonding band splitting, a property related to the local structure of the amorphous state. This discrepancy may have arisen because model structures of idealized, homogeneous, amorphous materials are of necessity used in theoretical work, and these will certainly differ to some extent from the ''true'' bulk structure. In addition, the bulk structure may not be a suitable model of the atomic structure of the surface and near-surface regions. Yet it is the electronic structure of these that is probed by the electron spectroscopic techniques used in this paper. Experimentally, of course, structural or compositional inhomogeneities, such as a mix of iron clusters and Fe-Y, may also be present in these sputter-grown alloy films and these could give rise to the observed valence band photoemission; however, the secondary electron behavior is not consistent with this.

The reduced average spin polarization of the valence band emission of $Fe_{60}Y_{40}$ compared with Fe is in accordance with the alloy exhibiting both a smaller exchange splitting (as predicted by theory) and a smaller Fe atom magnetic moment than in pure metal. However, the dominance of the majority-spin carriers at the Fermi edge is clearly contrary to current theories and calculations of the surface and near-surface spin-resolved DOS would be very valuable in resolving this anomaly. Sample inhomogeneity may be playing a role, with Fe-rich regions important for the polarization behavior, but this is not believed to be a major factor as the spin-resolved bands are distinctly different from those of polycrystalline Fe and the low-energy secondary electron polarization suggests an environment very different from that of Fe.

V. SUMMARY

Spin-resolved photoemission spectra have been measured from in situ sputtered Fe and Fe-Y alloys. From secondary electron spin hysteresis loops, $Fe_{60}Y_{40}$, but not $Fe_{41}Fe_{59}$, was found to order ferromagnetically at the lowest temperature accessible in our equipment, ~114 K. The spin-integrated valence band photoemission spectrum of $Fe_{60}Y_{40}$ shows little difference from that of pure Fe; however, the mean valence band polarization and the secondary electron polarizations of the two materials are very different. Contrary to calculated spin-resolved DOS, the majority-spin electrons of $Fe_{60}Y_{40}$ dominate the photoemission at the Fermi edge. The 1 eV secondary electron polarization of $Fe_{60}Y_{40}$ was found to be diminished rather than enhanced relative to the mean valence polarization, an effect that supports a predicted negative polarization of yttrium. This work demonstrates the importance of spin-resolved photoemission measurements in testing theoretical calculations of amorphous magnetic alloys. Furthermore, the successful combination of in situ sputtering and spin-resolved electron spectroscopy measurements opens the way for a broad range of experimental investigations of the spin-dependent electronic structure of magnetic amorphous alloys and granular materials.

ACKNOWLEDGMENTS

[1] C. Becker and J. Hafner, Phys. Rev. B **50**, 3913 (1994).

[2] M. Yu and Y. Kakehashi, J. Phys. Condens. Matter **8**, 5071 (1996).

[3] D. Spisak, C. Becker, and J. Hafner, Phys. Rev. B **51**, 11 616 (1995).

[4] H. J. Nowak, O. K. Anderson, T. Fujiwara, O. Jepson, and P. Vargas, Phys. Rev. B **44**, 3577 (1991).

[5] A. M. Bratkovsky and A. V. Smirnov, J. Phys. Condens. Matter **5**, 3203 (1993).

[6] H. Tanaka, S. Takayama, M. Hasegawa, T. Fukunaga, U. Mizutani, A. Fujita, and K. Fukamichi, Phys. Rev. B **47**, 2671 (1993).

[7] H. Hopster, R. Kurzawa, R. Raue, W. Q. Schmitt, G. Guntherodt, K. H. Walker, and H. J. Guntherodt, J. Phys. F **85**, L11 (1985).

[8] A. K. See and L. E. Klebanoff, J. Appl. Phys. **79**, 4796 (1996).

[9] Y. B. Xu, C. G. H. Walker, D. Greig, E. A. Seddon, I. W. Kirkman, F. M. Quinn, and J. A. D. Matthew, J. Phys. Condens. Matter **8**, 1567 (1996).

[10] J. Unguris, D. T. Pierce, A. Galejs, and R. J. Celotta, Phys. Rev. Lett. **49**, 72 (1982).

[11] Th. Paul and H. Neddermeyer, J. Phys. F **15**, 79 (1985).

[12] I. W. Kirkman, E. A. Seddon, and F. M. Quinn (unpublished).

[13] F. M. Quinn, E. A. Seddon, and I. W. Kirkman, Rev. Sci. Instrum. **66**, 1564 (1995).

[14] D. R. Penn, S. P. Apell, and S. M. Girvin, Phys. Rev. Lett. **55**, 518 (1985).

[15] Y. B. Xu, D. Greig, C. G. H. Walker, E. A. Seddon, and J. A. D. Matthew (unpublished).

[16] J. J. Yeh and I. Lindau, At. Data Nucl. Data Tables **32**, 1 (1985).

[17] J. M. D. Coey, D. Givord, A. Liénard, and J. P. Rebouillat, J. Phys. F **11**, 2707 (1981).

[18] J. J. Croat and J. F. Herbst, J. Appl. Phys. **53**, 2294 (1982).

[19] J. Chappert, J. M. D. Coey, A. Liénard, and J. P. Rebouillat, J. Phys. F **11**, 2727 (1981).

[20] T. VanZandt, R. Browning, and M. Landolt, J. Appl. Phys. **69**, 1564 (1991).

[21] K. O'Grady and R. W. Chantrell, *Studies of Magnetic Properties of Fine Particles* (Elsevier, Amsterdam, 1992), p. 93.

[22] S. Ishio, M. Fujikura, T. Ishii, and M. Takahashi, J. Magn. Magn. Mater. **60**, 236 (1986).

[23] M. Tenhover, D. Lukco, and W. L. Johnson, J. Non-Cryst. Solids **61&62**, 1049 (1984).

[24] G. A. N. Connell, S.-J. Oh, J. Allen, and R. Allen, J. Non-Cryst. Solids **61&62**, 1061 (1984).

[25] B. Sinkovic, E. Shekel, and S. L. Hulbert, Phys. Rev. B **52**, R8696 (1995).

[26] H. Hopster, Phys. Rev. B **36**, 2325 (1987).

[27] H. Tang, T. G. Walker, H. Hopster, D. P. Pappas, D. Weller, and J. C. Scott, J. Magn. Magn. Mater. **121**, 205 (1993).

[28] H. Tang, T. G. Walker, H. Hopster, D. P. Pappas, D. Weller, and J. C. Scott, Phys. Rev. B **47**, 5047 (1993).

[29] H. A. Mook and C. G. Shull, J. Appl. Phys. **37**, 1034 (1966).

[30] M. J. Cooper, D. Laundy, D. A. Cardwell, D. N. Timms, and R. S. Holt, Phys. Rev. B **34**, 5984 (1986).

[31] E. Kisker, W. Gudat, and K. Schroder, Solid State Commun. **44**, 591 (1982).

[32] R. Allenspach, M. Taborelli, M. Landolt, and H. C. Siegmann, Phys. Rev. Lett. **56**, 953 (1986).